

 <p>ISSN NO. 2320-5407</p>	<p>Journal Homepage: -www.journalijar.com</p> <h2>INTERNATIONAL JOURNAL OF ADVANCED RESEARCH (IJAR)</h2> <p>Article DOI:10.21474/IJAR01/11179 DOI URL: http://dx.doi.org/10.21474/IJAR01/11179</p>	
---	---	---

RESEARCH ARTICLE

REACTIVE NITROGEN SPECIES IN BRAIN AFTER IN VIVO EXPOSURE TO ARSENIC

Dr. Julián G. Bonetto^{1,2}, Dr. Juan C. Perazzo³ and Dr. Susana Puntarulo^{1,2}

1. Facultad de Farmacia y Bioquímica, Fisicoquímica-IBIMOL, Universidad de Buenos Aires, Buenos Aires, Argentina.
2. Instituto de Bioquímica y Medicina Molecular (IBIMOL), CONICET-Universidad de Buenos Aires, Buenos Aires, Argentina.
3. Laboratory of Hepatic Encephalopathy and Portal Hypertension, Center of Applied and Experimental Pathology, University of Buenos Aires, Buenos Aires, Argentina

Manuscript Info

Manuscript History

Received: 15 April 2020

Final Accepted: 18 May 2020

Published: June 2020

Key words:-

Arsenic, Brain, Oxidative Stress, Nitric Oxide, Nitrosative Stress

Abstract

Arsenic (As) is a natural pollutant, which exposure is related to a variety of diseases like hypertension, diabetes, cancer and neurodegenerative or neurodevelopment impairment but, the exact mechanism by which As exposure could be toxic is still unclear. Studies employing different models of Astoxicity suggested that As could cause ROS generation and antioxidant depletion in biological systems, including controversial data related to RNS generation and nitrosative damage. The hypothesis of the present work is that acute As exposure could trigger an imbalance in the production of RNS in brain, leading to nitrosative stress and nitrosative-dependent cellular damage. The effect of in vivo exposure to As was studied by histopathology of the tissue, NO_2^- plus NO_3^- content, NO generation rate employing Electron Paramagnetic Resonance (EPR) techniques, and the content of nitrotyrosine ($\text{NO}_2\text{-Tyr}$) of total proteins in rat brain by western blot techniques. The data presented here suggested that the exposure to As increased the production of NO and lipid radicals in brain, leading to nitrosative damage to proteins and a depletion of the hippocampal pyramidal cell layer, that could affect functionality of the brain.

Copy Right, IJAR, 2020. All rights reserved.

Introduction:-

Arsenic (As) is a natural metalloid affecting the health of millions of people worldwide by its uptake in the food and drinking water. Several reports indicate that the exposure to As resulted in a noxious effect on the central nervous system, both in early and adult life. These observations associated As presence with cognitive dysfunction and several behavior deficits in children (Signes-Pastor et al., 2019; Adedara et al., 2020) and Parkinson or Alzheimer disease, through neuro-inflammation and -degeneration in adulthood (Costa, 2019). As exposure was studied in a variety of in vitro, ex vivo and in vivo experimental models to understand the mechanisms of action of As deleterious effects. The role of oxidative stress in the changes associated to As presence was characterized by assaying antioxidant enzymes activities, such as superoxide dismutase (SOD), catalase (CAT), glutathione reductase (GR) and glutathione peroxidase (GPx) (Flora, 2011); and also glutathione (GSH) content and the activity of the enzyme heme-oxygenase (Thomas et al., 2004; Bharti et al., 2012; Negishi et al., 2013). Several reports of As exposure in cell lines and animals include the production of superoxide anion (O_2^-) and hydrogen peroxide (H_2O_2),

Corresponding Author:- Dr. Susana Puntarulo

Address:- Facultad de Farmacia y Bioquímica, Fisicoquímica-IBIMOL, Universidad de Buenos Aires, Buenos Aires, Argentina.

accompanied with a decrease in the activities of antioxidant enzymes. Even though, there is not an experimental model that resembles As human effects, Wang et al. (2002) summarized some successful studies using rats and mouses. Chandravanshi et al. (2018) reported that As exposure could enhance the oxidative stress in brain through the damage on the mitochondrial function and cell apoptosis in some brain regions. Recently, Bonetto et al. (2017) showed new evidence on the generation of specific radical species by As treatment, both using ex vivo and in vivo models. In this regard, the authors reported that oxidative stress, assessed as the ascorbyl radical (A^{\cdot})/ascorbate (AH) content ratio, in the hydrophilic cellular medium was not modified significantly by acute As exposure. However, in the lipophilic cellular environment, when the ratio lipid radical (RL^{\cdot})/ α -tocopherol (α -T) content was assessed to evaluate oxidative stress in the rat brain, the exposure to As showed significant increases. Also, the possibility that the specific triggering of some oxidative pathways (such as oxidation of GSH) occur accordingly to the via As reaches the brain, even achieving the same concentration of the toxic in the tissues, was pointed out (Bonetto et al., 2017).

As it was previously suggested by Bonetto et al. (2014), As could show, on top of oxidative effects, nitrosative stress through generation of reactive nitrogen species (RNS). Nitric oxide (NO) is a free radical and a neurotransmitter produced for a family of nitric oxide synthases (NOS) including an inducible NOS (iNOS), an endothelial NOS (eNOS) and a neuronal NOS (nNOS). The NO is a neuro-protector under optimal physiological steady state concentration. However, under stressful circumstances, it can be generated in excess and become neurotoxic (abdel Naseer et al., 2020). At this time, it is proposed that the main cause, at least for protein modification, is related to the reactive nitrogen species (RNS) production. These species are generated when NO reacts with O_2^- to form peroxynitrite ($ONOO^-$), a strong oxidant, that easily reacts with nucleophilic molecules (Alhalwani et al., 2020). If the production of NO is increased, the steady state concentration of $ONOO^-$ is also enhanced, and this situation could harm proteins via tyrosine (Tyr) nitration (Radi, 2018). Bharti et al. (2012) reported these alterations in cellular proteins along with increases in lipid peroxidation and decreases in GSH content in rat brain after exposure to As. Several conflicting reports concerning As-induced production of NO has been published (Jomova et al., 2011). Pachauri et al. (2013) suggested that chronic As exposure caused a significant increase in ROS followed by NO and calcium influx, with a significant role for mitochondrial driven apoptosis. As has also been found to initiate endothelial dysfunction by diminishing the integrity of vascular endothelium followed by inactivation of eNOS, which therefore reduces the generation and bioavailability of NO and increases oxidative stress (Ellinsworth, 2015). Goudarzi et al. (2018) and Saha et al. (2018) showed that the content of nitrite (NO_2^-) and nitrate (NO_3^-), as indicator of NO production, was increased in rat brain after As. These data are considered only an indirect approach to the NO generation, but few reports are available in the literature.

The hypothesis of the present work is that acute As exposure could trigger an imbalance in the production of RNS in brain, leading to nitrosative stress and nitrosative-dependent cellular damage. The effect of in vivo exposure to As was studied by histopathology of the tissue, NO_2^- plus NO_3^- content, NO generation rate employing EPR techniques, and the content of nitrotyrosine (NO_2 -Tyr) of total proteins in rat brain by western blot techniques.

Material and Methods:-

Experimental design:

The School of Pharmacy and Biochemistry, University of Buenos Aires, provided the male Albino Wistar rats (200 ± 20 g) used in this study through the Animal Facility. The animals were housed under standard conditions of light, temperature and humidity, with unlimited access to water and food. The rats were injected intraperitoneally (ip) with one dose of sodium arsenite ($NaAsO_2$) of 5.8 mg As/kg body weight. Saline solution was employed to sham-injected control rats. Brains from control and As-treated animals were excised from euthanized animals in a CO_2 chamber, and rinsed in cold saline solution. Except where noted otherwise, the samples were freeze-clamped immediately following removal and stored under liquid N_2 until used. Whole blood was taken by cardiac puncture. Experimental animal protocols and procedures were carried out in accordance with the Guide for the Care and Use of Laboratory Animals (1985) and according to the principles and directives of the European Communities Council Directives (1986). The procedures also received approval from the Institutional Animal Care and Use Committee-School of Pharmacy and Biochemistry, University of Buenos Aires (CICUAL-FFyB, RES N°1037).

As content

The quantification of As species [$As^V + As^{III} +$ monometillarsonic acid (MMA) + dimethyl arsinic acid (DMA)] content in brain and whole blood was performed by hydride generation-atomic absorption spectrometry (HG-AAS),

after dry mineralization. A hydride generator VGA77 and an atomic absorption spectrometer Varian Spectra AA 200 were employed according to Navoni et al. (2009).

Histopathology:

Immediately after sacrifice, brain samples were obtained and fixed for light microscopy and for high resolution light microscopy (HRLM). For light microscopy a routine fixation with formalin-buffered solution was used. For HRLM samples were fixed in glutaraldehyde 3% (v/v) in sodium cacodylate buffer 0.1 M (sodium cacodylate 2.14 g-distilled water 100 ml), post-fixed in osmium tetroxide (Palade solution: osmium tetroxide 1 g, distilled water 50 ml) in Caulfield buffer (Palade solution 20 ml and 0.9 g of sucrose) during 90 min. Then samples were washed with distilled water twice, stained in block with uranyl acetate 2% (v/v) for 2 h and then washed twice with distilled water. After dehydration with increased alcohol concentrations, tissues were included with propylene oxide-epoxy resin (propylene oxide 100%, propylene oxide epoxy resin 2:1, then 1:1 and finally 1:2 overnight treated). Fixed tissue was placed in beam capsules and cut with an Ultracut Reichert-Jung ultramicrotome and stained with toluidine solution and counter nuclear staining. For observation and photographs a Digital Pathology Slide Scanner Scope Leica Biosystems Aperio CS2 (USA) was used.

Determination of 2',7'-Dichlorofluorescein Diacetate (DCFH-DA) oxidation rate:

DCFH-DA oxidation was quantified by fluorescent according to Lebel et al., (1992) with modifications. Brain tissue (250 mg fresh weight (FW)/ml) was homogenized in 100 mM Tris-HCl buffer solution pH 7.2 with EDTA 2 mM and MgCl₂ 5 mM. The detection was performed using a Varioskan LUX microplate reader. The reaction mixture contain 8 µl of homogenate, 3 µl of 1 mg/ml DCFH-DA solution in pure methanol and 239 µl of HEPES buffer per well, in different time of incubation at 37°C. Samples fluorescence was determined at $\lambda_{ex}=488$ nm and $\lambda_{em}=525$ nm.

Detection of LR[•] generation rate by EPR:

LR[•] generation rate was detected by a spin trapping technique using N-t-butyl- α -phenyl nitron (PBN) according to Bonetto et al. (2017). Brain tissue was homogenized in DMSO-PBN 40 mM in a concentration of 25 mg of tissue per ml, incubated for 30 min and immediately transferred to a glass Pasteur pipette for LR[•] detection. Instrument settings were as follows: modulation frequency 50 kHz, microwave power 10 mW, microwave frequency 9.75 GHz, centered field 3487 G, time constant 81.92 ms, modulation amplitude 1.20 G and sweep width 100 G, according to Lai et al. (1986). Quantification of the spin adduct was performed using TEMPO introduced into the same sample cell used for spin trapping. EPR spectra for both sample and TEMPO solutions were recorded at the same spectrometer settings and the first derivative EPR spectra were double integrated to obtain the area intensity, then the concentration of spin adduct was calculated according to Kotake et al. (1996).

Nitrite (NO₂⁻) plus nitrate (NO₃⁻) content:

The content of NO₂⁻+NO₃⁻ was determined by the Griess reaction, following Miranda et al. (2001) using VCl₃ for reduced agent. The brain was homogenized in pure ethanol at -20°C for protein removal, in a concentration of 200 mg FW/ml. The brain homogenate was then incubated for 2 h at -20°C and was centrifuged for 10 min at 4000g and 4°C. The supernatant was recovery and it was added the Griess reagent which was incubated for 10 min. The NO₂⁻+NO₃⁻ content was measured spectrophotometrically at $\lambda=540$ nm. Quantification was done using standard curves of NO₂⁻ and NO₃⁻ in the range of 0 to 80 µM.

NO generation rate by EPR:

Rat brains tissue (750 mg FW/ml) was homogenized in presence of 10 mM MGD-Fe²⁺ (Fe-N-methyl-D-glucaminedithiocarbamate complex⁺) (10:1), as spin trap, in a 100 mM potassium phosphate buffer solution, pH = 7.4. NO generation was measured in a spectrophotometer Bruker ECS 106 band X, with a cavity ER 4102ST at room temperature. The measurements were performed using the following spectral parameters: modulation frequency: 50 kHz, microwave power: 20 mW, microwave frequency: 9.75 GHz, center field: 3400 G, time constant: 20.48 ms, sweep wide: 100 G and modulation amplitude: 5.983 G. The quantification of the NO content was performed using a 2,2,5,5-tetramethylpiperidine-1-oxil (TEMPO), according to Lai and Komarov(1994).

NO₂-Tyr content in total proteins of brain:

Protein was separated by reducing 10% (w/v) polyacrylamide gel electrophoresis (60 µg per street) and electroblotted to PVDF membranes. Membranes were blotted overnight in 5% (w/v) non-fat milk, and then incubated 2 h in the presence of the anti-NO₂-Tyr antibodies (ABCAM HM.11; 2 µg/15 ml) in 5% (w/v) bovine serum albumin in PBS buffer, containing 0.1% (v/v) Tween-20. After several washes with PBS buffer containing

0.1% (v/v) Tween-20, the membrane was incubated for 2 h at room temperature in the presence of the secondary antibody (HRP-conjugated). The conjugates were visualized by chemiluminescence detection in a Kodak medical X-Ray film with cumaric acid 0.2 M, luminol 1.25 M, H₂O₂ 0.06% (v/v) in Tris-HCl buffer 0.1 M pH 8.8.

Protein content

Quantification of proteins was performed according to Lowry (1951), employing bovine serum albumin (BSA) as standard.

Statistical analyses

Data in the text and tables are expressed as mean values \pm standard error of the mean (S.E.M.). Statistical tests were carried out using Graph Pad Prism 6, one-way ANOVA with Dunnett's post-test, with a level of statistical significance of $p < 0.05$.

Results:-

The distribution of total As content in blood and brain in this model of acute intoxication in rats treated with a unique ip dose (5.8 mg As/kg body weight), was measured as a function of time post As administration (Table 1). Both, in blood and brain, a significant increase in As content was observed after 4 h, as compared to control animals, that is maintained at least over 31 h post treatment.

Table 1:- Arsenic content in blood and brain tissues.

Time	As content in blood (nmol As/ml)	As content in brain (pmolAs/mg FW)	Total As in blood (μ g)	Total As in brain (μ g)
Control	10 \pm 1	n.d.	10 \pm 1	n.d.
4 h	187 \pm 12*	4 \pm 2*	179 \pm 12*	0.45 \pm 0.07*
8 h	344 \pm 42*	6.6 \pm 0.9*	330 \pm 40*	0.81 \pm 0.12*
16 h	326 \pm 21*	4.4 \pm 0.3*	312 \pm 20*	0.55 \pm 0.04*
24 h	400 \pm 16*	4 \pm 1*	384 \pm 16*	0.55 \pm 0.13*
31 h	393 \pm 18*	6.7 \pm 0.9*	376 \pm 17*	0.80 \pm 0.11*

*significant different as compared with control, $p < 0.05$.

Data in figure 1 show the histopathology performed using HRLM of brain slices stained with haematoxylin-eosin of rat brain from control animals and from rats 24 h post i.p. injection with 5.8 mg As/kg. The obtained results showed disarrangement in the pyramidal cell layer of the hippocampal with a decrease in the number of pyramidal neurons in brains from animals exposed to As.

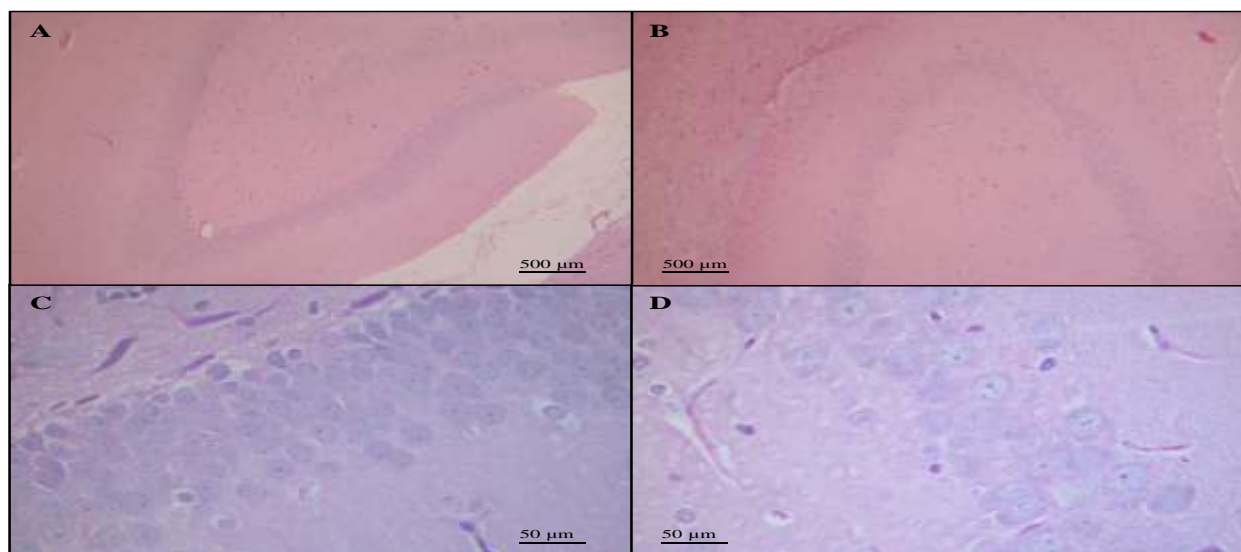


Figure 1:- HRLM in brain slices stained with haematoxylin-eosin. **A.** Control rat brain (63x); **B.** Rat brain at 24 h post i.p. injection with 5.8 mg As/kg FW (63x); **C.** Control rat brain (630x); **D.** Rat brain at 24 h post i.p. injection with 5.8 mg As/kg FW (630x).

An assay using DCFH-DA oxidation was employed to assess ROS production in brain homogenates. Data on figure 2A show the increase in DCFH-DA oxidation as a function of the incubation time during the experimental assay. Non-significant changes in the DCFH-DA oxidation rate was observed in brain homogenates from As treated rats, as compared to values in control brains (Fig. 2A).

Lipid peroxidation was assessed by an EPR technique detecting the presence of LR[•] combined with the spin trap PBN that resulted in adducts that gave a characteristic EPR spectrum with hyperfine coupling constants of $a_N = 15.8$ G and $a_H = 2.6$ G, in agreement with computer simulated signals obtained using those parameters (Fig. 2B, trace a). According to Buettner (1987) these constants could be assigned to LR[•], however, spin trapping studies cannot distinguish between peroxy (ROO[•]), alkoxy (RO[•]) and alkyl (R[•]) adducts, since the coupling constants are too similar to be differentiated. PBN by itself was examined and no PBN spin adduct was observed (Fig. 2B, trace b). The generation rate of LR[•] adducts in control brain homogenates (Fig. 2B, trace c) was increased by 3-fold in brain samples from rats treated 24 h before with one dose of As (Fig. 2B, trace d). Quantification of the EPR signals is shown in figure 2B insert.

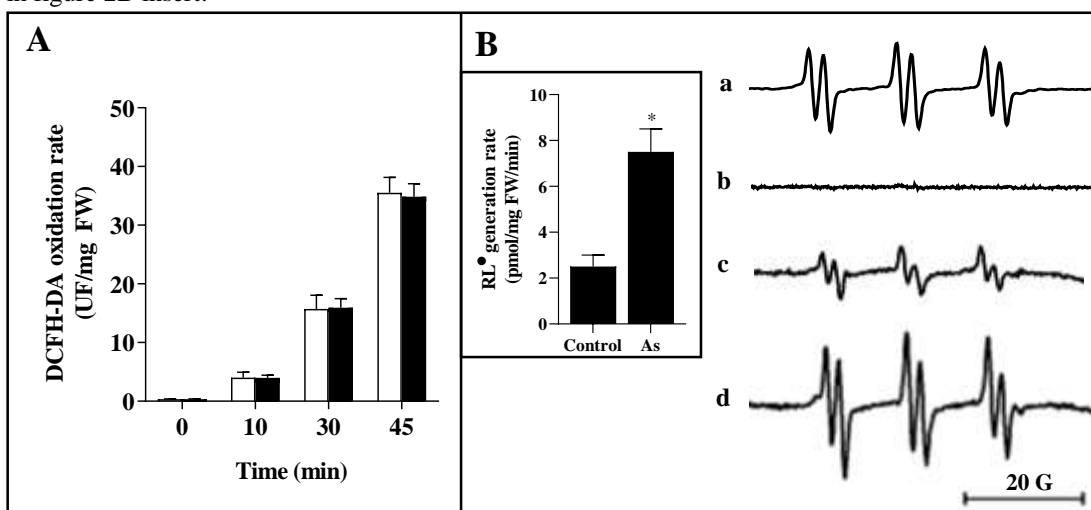


Figure 2:- Oxidative status in brain after exposure to a i.p dose of 5.8 mg As/kg of body weight. **A.** DCFH-DA oxidation rate as function of the incubation time during the experimental assay. **B.** EPR spectrum for LR[•] in brain: a) computer simulated-spectrum, b) PBN alone, c) spectrum of LR[•] in control brain rat, d) spectrum of brain rat 24 h post-injection with As.*significant different as compared with control, $p < 0.05$.

As an initial estimation of the RNS generation in rat brain, the content of NO_2^- and NO_3^- was measured. Data in figure 3 showed that, both NO_3^- and total NO_x content, was significantly decreased by As administration with no significant changes in the content of NO_2^- in rat brain at 24 h post i.p. injection with 5.8 mg As/kg.

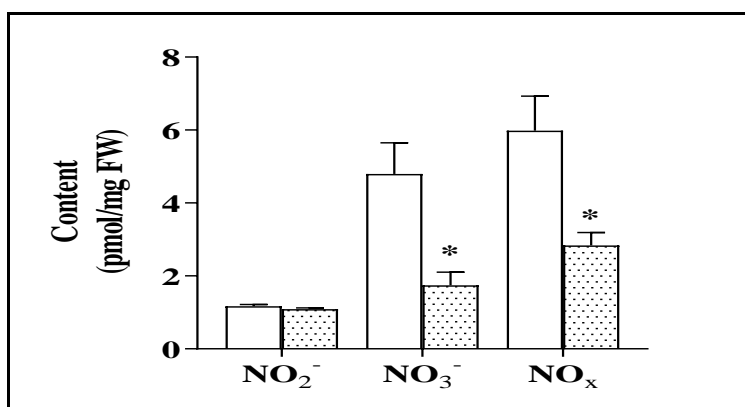


Figure 3:- Content of NO_2^- , NO_3^- and total nitrates (NO_x) in rat brain. The content of these parameters was assessed in control rat brain (□) and in rat brain isolated from animals 24 h post i.p. injection with 5.8 mg As/kg of body weight (▨).*significant different as compared with control, $p < 0.05$.

To further identify the production of NO by rat brain homogenates, the detection of NO was performed employing EPR assays. Control rat brains showed a distinctive EPR signal for the adduct MGD-Fe-NO ($g = 2.03$ and $a_N = 12.5$ G) that increased with tissue weight (Fig. 4A). The EPR signal for NO content in homogenate control rat brain incubated for 30 min at 37°C was assessed as indicated in Material and Methods section and, compared to the computer simulated-spectrum. The NO content in homogenates from rat brain incubated for 30 min depended on the tissue weight (Fig. 4B). Figure 4C showed that NO content in 200 mg of homogenate control rat brain significantly increased as a function of the incubation time. The administration to the animals of a single i.p. dose of 5.8 mg As/kg body weight significantly increased the NO generation rate, assessed by the EPR signal depended on NO-MGD-Fe²⁺, after 24 h of administration of As (Fig. 5).

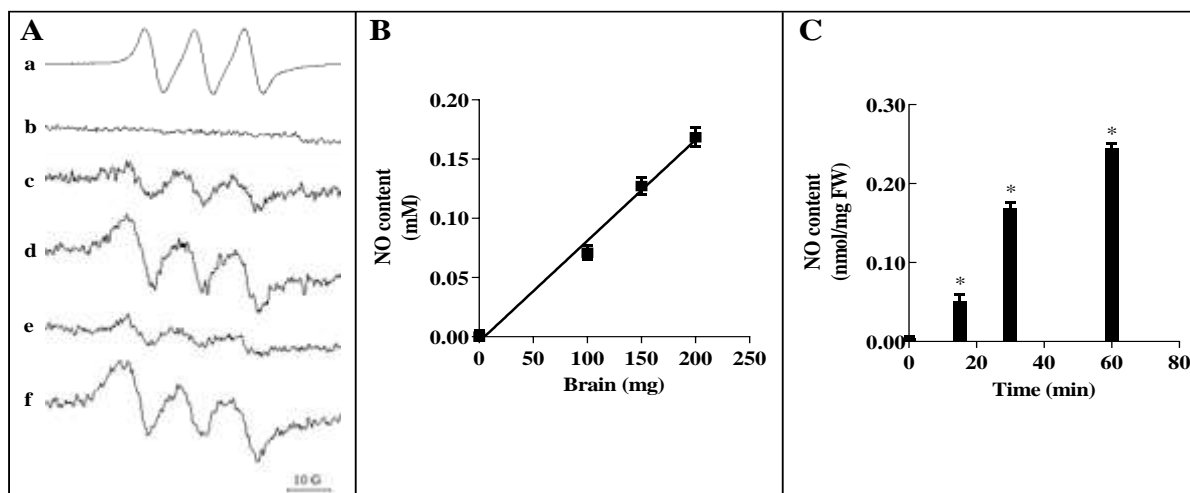


Figure 4:- NO content assessed by EPR as function of time and tissue weight. **A.** EPR signal for NO content in homogenate control rat brain incubated at 37°C, a) computer simulated-spectrum, b) MGD-Fe²⁺ complex by itself, c) NO-MGD-Fe²⁺ spectrum of 100 mg homogenate rat brain incubated for 30 min, d) NO-MGD-Fe²⁺ spectrum of 200 mg of tissue incubated for 30 min, e) NO-MGD-Fe²⁺ spectrum of 200 mg of tissue incubated for 15 min, f) NO-MGD-Fe²⁺ spectrum for 200 mg of tissue incubated for 60 min. **B.** Quantification of NO content in homogenate of rat brain incubated for 30 min as function of tissue weight. **C.** Quantification of NO content in 200 mg of homogenate of rat brain isolated from control animals as a function of the incubation time. *significant different as compared with control, $p < 0.05$.

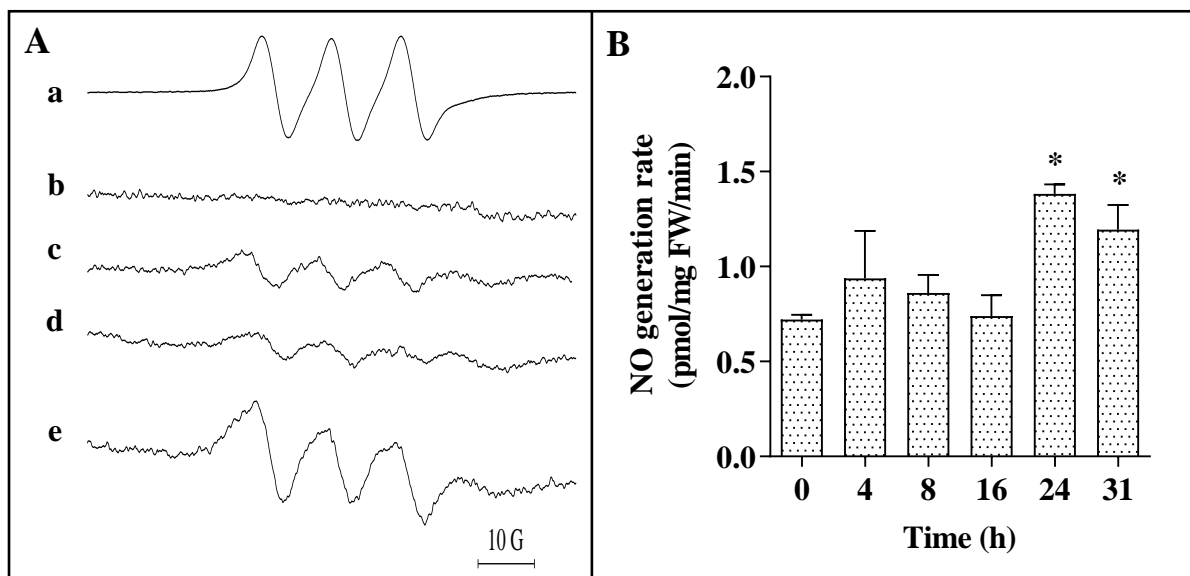


Figure 5: NO generation rate in brain after As exposure. **A.** EPR signal for NO content in brain isolated from control and As-exposed rats (single i.p. dose of 5.8 mg As/kg of body weight). a) computer simulated-spectrum, b) MGD-

Fe²⁺ complex by itself, c) NO-MGD-Fe²⁺ spectrum of brain samples isolated from control rats, d) NO-MGD-Fe²⁺ spectrum of brain samples isolated from rats after 16 h of As administration, e) NO-MGD-Fe²⁺ spectrum of brain samples isolated from rats after 24 h of As administration. **B.** Quantification of NO generation rate in brain after of exposure to As. *significant different as compared with control, p<0.05.

Moreover, the NO₂-Tyr content in the proteins of the brain homogenates was measured by western blot experiments. Data in figure 6 showed a significant increase by 92% after 24 h in brains of animals receiving a single dose of 5.8 mg As/kg, as compared to brains from control animals.

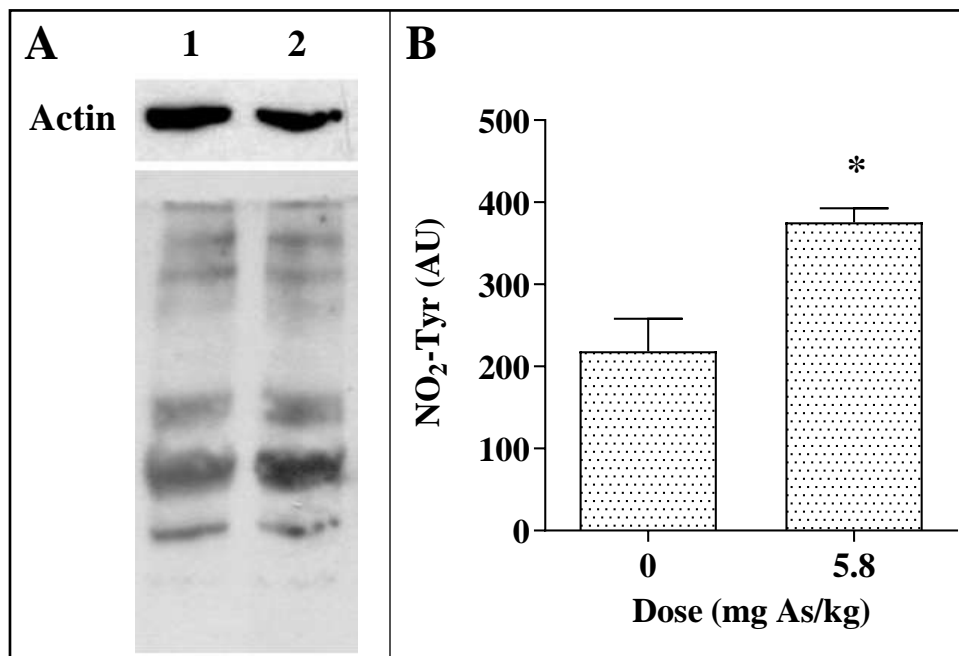


Figure 6: Protein nitration in brain after As exposure. **A.** Western-blot using anti-NO₂-Tyr antibody. **Lane 1,** Nitrate protein in control rat brain. **Lane 2,** Nitrate protein in As exposure rat brain. **B.** Quantification of NO₂-Tyr content in brain. *significant different as compared with control, p<0.05.

Discussion:-

The brain is the more complex organ in the body of the vertebrates, and even though it is protected by the skull and the meninges, suspended and surrounding by the cerebrospinal fluid and isolated from the circulatory system by the blood brain barrier (BBB) (Khonsary, 2017), the nature and complexity of the brain makes it very vulnerable to damage by toxic agents. The tested model of in vivo exposure to As in rats was consistent with previous studies, in terms of the concentration of As reached in blood and brain after a single dose ip of 5.8 mg As/kg body weight (Bonetto et al., 2017). The content of As was low, but detectable by the experimental technique used in this study, in blood of control rats. However, non-detectable amounts of As were found in control brain of these animals. The kinetic data included here showed that over the initial 31 h post administration of As to the rats, the As content in brain was not significantly different, and represents 0.25% and 0.22% after 4 h and 31 h, respectively, of the total content in blood.

It is widely accepted that severe and moderate As intoxication could be responsible for acute encephalopathy included peripheral neuropathy, cognitive decline and delirium, convulsions, paralysis, coma and even death (Morton and Caron 1989; Jha et al., 2002). On the other hand, Gong and O'Bryant(2010) suggested the likely relationship between the exposure to As and the development of neurological pathologies, such as Alzheimer disease. However, the neurotoxic effects and the mechanisms of the neurotoxicity processes triggered by the exposure to As are almost unknown until now (Chandravanshi et al., 2018). Among the main brain areas, it should be mentioned the hypothalamus, the brain cortex, the corpus striated and the hippocampus, as the areas that are described to be in charge of important functions such as the memory, the attention, the perception, the language, the awareness, the emotions and the motricity (Kandel, 2013). Von Bartheld et al. (2016) reported a link between the

lost in the number of neuronal cells and the development of neurodegenerative diseases. Chen et al. (2020) report a decrease of 20 to 35% of the total volume and cell number of the hippocampal in subject with schizophrenia and depression. Chandravanshi et al. (2018) reported a neurotoxic effect through ROS generation and oxidative stress driven mitochondrial dysfunction and cell death by neural apoptosis in frontal cortex, hippocampus and corpus striatum of developing rat exposed to As. Postnatal exposure to As revealed an impair in learning and memory in rats which it is alleviate with the supplementation of α -lipoic acid, an important lipophilic antioxidant of the CNS with the ability of cross the BBB, restore the intracellular GSH and preserve the hippocampal neuronal morphology (Dixit et al., 2020). The disarrangement in the pyramidal cell layer of the hippocampal with a decrease in the number of pyramidal neurons reported here, after 24 h of the single dose of As, is consistent with morphological alterations in the histology of the brain by As exposure. These histological alterations should be reflected in the deterioration of cellular functions in the brain.

The DCFH-DA oxidation rate is a global indicator in of ROS production the brain, mostly in the hydrophilic cellular environment. The lack of effect on this parameter suggested that, in agreement with previous observations employing this model assessing the A/AH⁻ content ratio (Bonetto et al., 2017), the hydrophilic medium is not particularly affected by exposure to As. However, the LR⁺ generation rate by treated animals brain tissue, showed a significant increase, as compared to the control group. This observation suggested that severe effect on the membranes resulting in lipid deterioration is an important consequence of As administration, in agreement with previously shown data (Bonetto et al., 2017).

Jomova and Valko (2011) suggested that the exposure to As not only generates ROS, but RNS as well, leading to membrane and DNA damage. However, controversial results have been reported by Shi et al. (2004). In other study, SOD, CAT, different ROS scavengers and NOS inhibitors were evaluate in As exposure cells (Lynn et al., 2000). The result suggested that ROS, but no NO, are involved in As induced DNA strand break (Lynn et al., 2000). Jomova et al. (2011) reported in hepatocytes and human liver cells that NO₃⁻ and NO₂⁻ content was not changed in cells exposed to As. Moreover, Pi et al., (2000) measured a decrease in the content of NO₃⁻ and NO₂⁻, and a lower activity of the eNOS in human umbilical vein endothelial cells caused by As^{III} or As^{IV} in serum of human blood of a China population exposed to As through drinking water. Decreased level of NO₂⁻, NO₃⁻ and NOS activity was also reported in striatum of rat chronically exposed to As, accompanied by significant higher levels of lipid peroxidation and ROS production, as compared to control animals (Zarazúa et al., 2006). In the study presented here the NO₃⁻ content decreased after exposure to As. This effect could not be a direct reflection of NO content, since As is able to form a complex with NO and Fe or with As. For example, the decrease in the measured content of NO₃⁻ could be due to the formation of a Fe-N¹⁵-arsenate complex. McDonald et al. (1965) reported the generation of this complex in the presence of As by the measurement of an EPR spectrum with nine hyperfine components, consistent with hyperfine splitting by two equivalent N¹⁵ nuclei and two equivalent As⁷⁵ (I = 3/2) nuclei with both N¹⁵ and As⁷⁵ exhibiting coupling constants of about 3 gauss. Moreover, other studies employing EPR performed by Chevrier and Brownstein (1980) showed the generation of As complexes between NO₂⁻ and NO₃⁻ with AsF₆⁻ y AsF₃⁻. Also, NO₃⁻ is an anion that could be excluded from the brain to the main circulation blood through anion channels in the membranes. The combination of all or some of these possible reactions could lead to a decrease in the content of NO₂⁻ and NO₃⁻ in the brain that could not be due to a decrease in NO brain content. Thus, a high sensitivity technique to assess NO content, such as the direct measurement of NO by EPR, is information of critical value. In spite of the reported lack of change in the production of RNS after low exposure to As (lower than 5 μ M of As^{III}) of vascular endothelial cells using carboxy-PTIO as spin trap for NO (Barchowsky et al., 1999), in the study presented here a significant increased of NO was shown in the brain of the rats receiving As, suggesting the importance of the characteristics of the tissues/organ under study when analyzing the As effects.

Ferrer-Sueta et al. (2018) described that Tyr nitration is a two-step free radical-mediated process. It begins with the one-electron oxidation of the phenolic ring of Tyr to produce the tyrosyl radical (Tyr[•]), which then reacts with nitrogen dioxide ([•]NO₂) in a radical-radical coupling reaction to produce the nonradical product NO₂-Tyr. It is also suggested that many ONOO⁻ derived radicals can mediate the oxidation of Tyr to Tyr[•], such as [•]OH (Solar et al., 1984) and [•]NO₂ (Prütz et al., 1985) produced by peroxynitrous acid homolysis, carbonate (CO₃⁻) formed as a secondary product of the reaction of ONOO⁻ with CO₂ (Gow et al., 1996) and several oxo-metal complexes (O=Me⁽ⁿ⁺¹⁾⁺X), formed after the reaction between ONOO⁻ and certain transition metal centers (Ramezani et al., 1996). Moreover, in hydrophobic environments, the one-electron oxidation of Tyr can also be mediated by some of the intermediates of lipid peroxidation processes, such as ROO[•] (Bartesaghi et al., 2010) and RO[•] (Folkes et al.,

2012) radicals, contributing thereby to protein Tyr nitration in lipid bilayers and lipoproteins. In vivo, there are several reactions that compete with the oxidation of Tyr, tending thus to inhibit Tyr nitration (Ferrer-Sueta et al., 2018). Not only the reactive species that oxidize Tyr can be consumed by many other targets but also several biological reductants, like GSH (Folkes et al., 2011), uric acid (Hunter et al., 1989) and AH^- (Hunter et al., 1989) can mediate repair reactions of the Tyr \cdot , reducing them back to Tyr and preventing its recombination with $\cdot\text{NO}_2$. In addition, α -tocopherol inhibits the formation of both, ROO^\cdot radicals and Tyr nitration (Bartesaghi and Radi, 2018). Higher yields of Tyr nitration can be produced when the one-electron oxidants and $\cdot\text{NO}_2$ arise through the direct reaction of ONOO^- with free or protein bound transition metal centers (Ferrer-Sueta et al., 2018). The one-electron reduction of ONOO^- with several low molecular weight transition metal complexes or certain heme peroxidases can form $\text{O}=\text{Me}^{(n+1)+}\text{X}$ and $\cdot\text{NO}_2$ almost quantitatively. ONOO^- seems as the most widespread nitrating species responsible for protein Tyr nitration in vivo, but Tyr nitration could also occur through ONOO^- -independent pathways, being the most relevant of these, the ones dependent on heme peroxidases activity. In this case, nitration requires the formation of strong one-electron oxidants by the reaction of hydrogen peroxide (H_2O_2) with several heme peroxidases (i.e., heme peroxidases compounds I and II); these species mediate both the oxidation of Tyr residues to Tyr \cdot and the one-electron oxidation of NO_2^- to $\cdot\text{NO}_2$, leading to the formation of $\text{NO}_2\text{-Tyr}$ (Marquez and Dunford, 1995). The increase content of nitrated proteins in the brain of As treated animals could be due to the reaction between either (a) ONOO^- , or (b) LR^\cdot , or (c) a combination of the reaction of both species. Since O_2^- formation seems to be increased after As treatment, as suggested previously (Jeong et al., 2017) and NO generation is increased, as shown here, ONOO^- is a suitable candidate for the increase in brain protein nitration. However, since LR^\cdot generation rate is also increased, this contribution should not be discarded. Thus, a combination of both species might participate in the increased content of $\text{NO}_2\text{-Tyr}$ in rat brain exposed to As.

The main features of the brain, such as the high content of polyunsaturated fatty acids (Khan & He, 2017), the high energy (above 20%) and O_2 consumption per weight unit (Karthikeyan et al., 2019), and the lack of a strong antioxidant capacity (Floyd, 1999) makes it possible that both, ROS and RNS, contribute strongly to the As-dependent damage after acute exposure.

Conclusion:-

The diagram shown in figure 7 briefly summarized the postulated integration of the results presented here. As is known to produce ROS but also O_2^- , singlet oxygen ($^1\text{O}_2$), ROO^\cdot , and H_2O_2 affecting the redox balance in the hydrophobic cellular environment (Bonetto et al., 2017). However, the exact mechanism responsible for the generation of these reactive species is not yet clear. Moreover, some studies proposed the formation of intermediary arsine species, dimethylarsinic peroxy radicals ($(\text{CH}_3)_2\text{AsOO}^\cdot$) and also the dimethylarsinic radical $(\text{CH}_3)_2\text{As}^\cdot$. For example, Flora et al. (2008) reported radical species generated by As exposure that were detected by analysis using EPR techniques. These species included $(\text{CH}_3)_2\text{AsOO}^\cdot$, as a product of dimethylarsine and O_2 reactions and this $(\text{CH}_3)_2\text{AsOO}^\cdot$ is assumed to play a major role in DNA damage, and may produce O_2^- during the process. However, in rat brain this is a new piece of direct evidence obtained by EPR in vivo showing that NO is significantly increase after a single dose of As. As it was previously stated, ONOO^- is formed from the reaction between NO and O_2^- and, due to the increase in NO and ROS, along with the As-derived radicals among others radicals, lead to an increase in the damage to lipids, DNA and proteins, as compared to brains isolated from control rats. In agreement with this hypothesis, significant increases in LR^\cdot and $\text{NO}_2\text{-Tyr}$ content in treated brains has been shown. This complex scenario, shows a clear increase in the steady state concentration of both, ROS and RNS, in rat brain after a single dose of As. Moreover, some clinical information reported that antioxidant levels in plasma from individuals exposed to As (Wu et al., 2006) were decreased and there was a significant inverse correlation between plasma antioxidant capacity and As concentration in whole blood. Thus, it could be promising to face clinical studies with pre-existing or newer chelating agents in order to understand the mechanism underlying the beneficial effects of antioxidants, and to explore optimal dosage and duration of treatment, in order to increase clinical recoveries in cases of humans exposed to As intoxication.

Future studies should be developed employing sensitive and specific techniques, such as those used here, to explore the participation of RNS in chronic As exposure to optimize therapeutic approach in cases of, for example, individuals living in areas receiving water containing As.

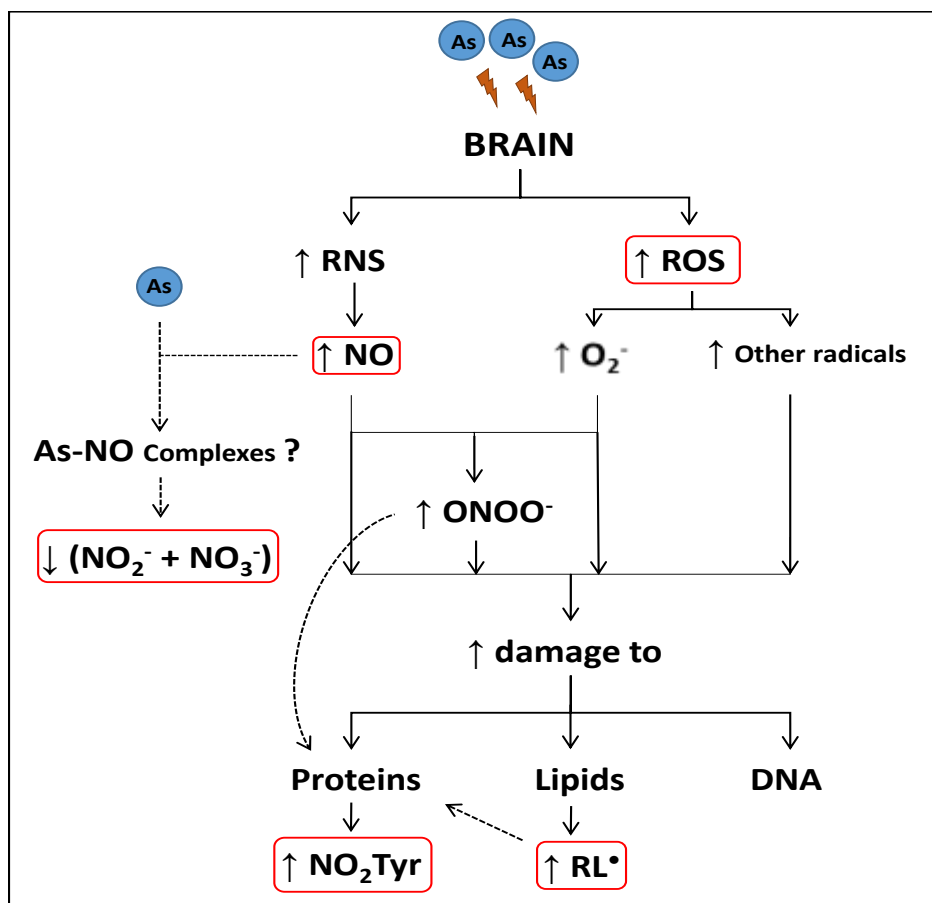


Figure 7:- Brief summary of the effects of the generation of ROS and RNS in rat brain after exposure to As. The parameters in red show the measurements reported here.

Acknowledgements:-

This study was supported by grants from the University of Buenos Aires (20020130100383BA), and CONICET (PIP N°11220170100539CO). SP is career investigator (CIC) from CONICET.

References:-

1. Abdel-Naseer, M., Rabah, A. M., Rashed, L. A., Hassan, A., & Fouad, A. M. (2020). Glutamate and Nitric Oxide as biomarkers for disease activity in patients with multiple sclerosis. *Mult. Scler. Relat. Disord.*, 38, 101873. <https://doi.org/10.1016/j.msard.2019.101873>
2. Adedara, I. A., Fabunmi, A. T., Ayenitaju, F. C., Atanda, O. E., Adebawale, A. A., Ajayi, B. O., Owoeye, O., Rocha, J. B. T., & Farombi, E. O. (2020). Neuroprotective mechanisms of selenium against arsenic-induced behavioral impairments in rats. *Neurotoxicology*, 76, 99-110. <https://doi.org/10.1016/j.neuro.2019.10.009>
3. Alhalwani, A. Y., Davey, R. L., Kaul, N., Barbee, S. A., & Alex Huffman, J. (2020). Modification of lactoferrin by peroxynitrite reduces its antibacterial activity and changes protein structure. *Proteins: Struct., Funct., Bioinf.*, 88(1), 166–174. <https://doi.org/10.1002/prot.25782>
4. Barchowsky, A., Klei, L. R., Dudek, E. J., Swartz, H. M., & James, P. E. (1999). Stimulation of reactive oxygen, but not reactive nitrogen species, in vascular endothelial cells exposed to low levels of arsenite. *Free Radical Biol. Med.*, 27(11–12), 1405–1412. [https://doi.org/10.1016/S0891-5849\(99\)00186-0](https://doi.org/10.1016/S0891-5849(99)00186-0)
5. Bartesaghi, S., & Radi, R. (2018). Fundamentals on the biochemistry of peroxynitrite and protein tyrosine nitration. *Redox Biol.*, 14, 618–625. <https://doi.org/10.1016/j.redox.2017.09.009>
6. Bartesaghi, S., Wenzel, J., Trujillo, M., López, M., Joseph, J., Kalyanaraman, B., & Radi, R. (2010). Lipid peroxyl radicals mediate tyrosine dimerization and nitration in membranes. *Chem. Res. Toxicol.*, 23(4), 832–835. <https://doi.org/10.1021/tx900446r>
7. Bharti, V. K., Srivastava, R. S., Sharma, B., & Malik, J. K. (2012). Buffalo (*bubalus bubalis*) epiphyseal

- proteins counteract arsenic-induced oxidative stress in brain, heart, and liver of female rats. *Biol. Trace Elem. Res.*, 146(2), 224–229. <https://doi.org/10.1007/s12011-011-9245-0>
8. Bonetto, J. G., Villaamil Lepori, E., & Puntarulo, S. (2017). Oxidative balance in brain after exposure to arsenic in ex vivo and in vivo models. *Int. J. Adv. Res.*, 5(10), 45–51. <https://doi.org/10.21474/IJAR01/5505>
 9. Bonetto, J. G., Villaamil Lepori, E., & Puntarulo, S. (2014). Update on the oxidative stress associated with arsenic exposure. *Curr. Top. Toxicol.*, 10, 37–48.
 10. Chandravanshi, L. P., Gupta, R., & Shukla, R. K. (2018). Developmental Neurotoxicity of Arsenic: Involvement of Oxidative Stress and Mitochondrial Functions. *Biol. Trace Elem. Res.*, 186(1), 185–194. <https://doi.org/10.1007/s12011-018-1286>
 11. Chen, F., Bertelsen, A. B., Holm, I. E., Nyengaard, J. R., Rosenberg, R., & Dorph-Petersen, K. A. (2020). Hippocampal volume and cell number in depression, schizophrenia, and suicide subjects. *Brain Res.*, 1727, 146546. <https://doi.org/10.1016/j.brainres.2019.146546>
 12. Chevrier, P. J., & Brownstein, S. (1980). Complex fluoroanions in solution-X. Complexes of phosphorus and arsenic fluorides with simple anions. *J. Inorg. Nucl. Chem.*, 42(10), 1397–1405. [https://doi.org/10.1016/0022-1902\(80\)80103](https://doi.org/10.1016/0022-1902(80)80103)
 13. Costa, M. (2019). Review of arsenic toxicity, speciation and polyadenylation of canonical histones. *Toxicol. App. Pharmacol.*, 375, 1–4. <https://doi.org/10.1016/j.taap.2019.05.006>
 14. Dixit, S., Mehra, R. D., & Dhar, P. (2020). Effect of α -lipoic acid on spatial memory and structural integrity of developing hippocampal neurons in rats subjected to sodium arsenite exposure. *Environ. Toxicol. Pharmacol.*, 75, 103323. <https://doi.org/10.1016/j.etap.2020.103323>
 15. Ellinsworth, D. C. (2015). Arsenic, Reactive Oxygen, and Endothelial Dysfunction. *J. Pharmacol. Exp. Ther.*, 353(3), 458–464. <https://doi.org/10.1124/jpet.115.223289>
 16. Ferrer-Sueta, G., Campolo, N., Trujillo, M., Bartesaghi, S., Carballal, S., Romero, N., Alvarez, B., & Radi, R. (2018). Biochemistry of Peroxynitrite and Protein Tyrosine Nitration. *Chem. Rev.*, 118(3), 1338–1408. <https://doi.org/10.1021/acs.chemrev.7b00568>
 17. Flora, S. J. S. (2011). Arsenic-induced oxidative stress and its reversibility. *Free Radical Biol. Med.*, 51(2), 257–281. <https://doi.org/10.1016/j.freeradbiomed.2011.04.008>
 18. Floyd, R. A. (1999). Antioxidants, Oxidative Stress, and Degenerative Neurological Disorders. *Proc. Soc. Exp. Biol. Med.*, 222(3), 236–245. <https://doi.org/10.1046/j.1525-1373.1999.d01-140.x>
 19. Folkes, L. K., Bartesaghi, S., Trujillo, M., Radi, R., & Wardman, P. (2012). Kinetics of oxidation of tyrosine by a model alkoxyl radical. *Free Radical Res.*, 46(9), 1150–1156. <https://doi.org/10.3109/10715762.2012.695868>
 20. Folkes, L. K., Trujillo, M., Bartesaghi, S., Radi, R., & Wardman, P. (2011). Kinetics of reduction of tyrosine phenoxyl radicals by glutathione. *Arch. Biochem. Biophys.*, 506(2), 242–249. <https://doi.org/10.1016/j.abb.2010.12.006>
 21. Gong, G., & O'Bryant, S. E. (2010). The Arsenic Exposure Hypothesis for Alzheimer Disease. *Alz. Dis. Assoc. Dis.*, 24(4), 311–316. <https://doi.org/10.1097/WAD.0b013e3181d71bc7>
 22. Goudarzi, M., Amiri, S., Nesari, A., Hosseinzadeh, A., Mansouri, E., & Mehrzadi, S. (2018). The possible neuroprotective effect of ellagic acid on sodium arsenate-induced neurotoxicity in rats. *Life Sci.*, 198, 38–45. <https://doi.org/10.1016/j.lfs.2018.02.022>
 23. Gow, A., Duran, D., Thom, S. R., & Ischiropoulos, H. (1996). Carbon Dioxide Enhancement of Peroxynitrite-Mediated Protein Tyrosine Nitration. *Arch. Biochem. Biophys.*, 333(1), 42–48. <https://doi.org/10.1006/abbi.1996.0362>
 24. Hunter, E. P. L., Desrosiers, M. F., & Simic, M. G. (1989). The effect of oxygen, antioxidants, and superoxide radical on tyrosine phenoxyl radical dimerization. *Free Radical Biol. Med.*, 6(6), 581–585. [https://doi.org/10.1016/0891-5849\(89\)90064-6](https://doi.org/10.1016/0891-5849(89)90064-6)
 25. Jeong, C. H., Seok, J. S., Petriello, M. C., & Han, S. G. (2017). Arsenic downregulates tight junction claudin proteins through p38 and NF- κ B in intestinal epithelial cell line, HT-29. *Toxicology*, 379, 31–39. <https://doi.org/10.1016/j.tox.2017.01.011>
 26. Jha, S., Dhanuka, A. K., & Singh, M. N. (2002). Arsenic poisoning in a family. *Neurol. India*, 50(3), 364–365. <http://www.ncbi.nlm.nih.gov/pubmed/12391471>
 27. Jomova, K., Jenisova, Z., Feszterova, M., Baros, S., Liska, J., Hudecova, D., Rhodes, C. J., & Valko, M. (2011). Arsenic: Toxicity, oxidative stress and human disease. *J. Appl. Toxicol.*, 31(2), 95–107. <https://doi.org/10.1002/jat.1649>
 28. Jomova, K., & Valko, M. (2011). Advances in metal-induced oxidative stress and human disease. *Toxicology*, 283(2–3), 65–87. <https://doi.org/10.1016/j.tox.2011.03.001>
 29. Kandel, E. R., Schwartz, J. H., & Jessell, T. M. (2013). *Principles of Neural Science 5th Ed.* McGraw-Hill, New

- York. <https://doi.org/0071390111>
30. Karthikeyan, S., Fiksenbaum, L., Grigorian, A., Lu, H., MacIntosh, B. J., & Goldstein, B. I. (2019). Normal Cerebral Oxygen Consumption Despite Elevated Cerebral Blood Flow in Adolescents With Bipolar Disorder: Putative Neuroimaging Evidence of Anomalous Energy Metabolism. *Front. Psychiatry*, 10, 739. <https://doi.org/10.3389/fpsy.2019.00739>
 31. Khan, M. Z., & He, L. (2017). The role of polyunsaturated fatty acids and GPR40 receptor in brain. *Neuropharmacology*, 113, 639–651. <https://doi.org/10.1016/j.neuropharm.2015.05.013>
 32. Khonsary, S. (2017). Guyton and Hall: Textbook of Medical Physiology. *Surg. Neurol. Int.*, 8(1), 275. https://doi.org/10.4103/sni.sni_327_17
 33. Kotake, Y., Tanigawa, T., Tanigawa, M., Ueno, I., Allen, D. R., & Lai, C.S. (1996). Continuous monitoring of cellular nitric oxide generation by spin trapping with an iron-dithiocarbamate complex. *Biochim. Biophys. Acta*, 1289(3), 362–368. [https://doi.org/10.1016/0304-4165\(95\)00172-7](https://doi.org/10.1016/0304-4165(95)00172-7)
 34. Lai, C. S., & Komarov, A. M. (1994). Spin trapping of nitric oxide produced in vivo in septic-shock mice. *FEBS Lett.*, 345(2–3), 120–124. [https://doi.org/10.1016/0014-5793\(94\)00422-6](https://doi.org/10.1016/0014-5793(94)00422-6)
 35. Lai, E. K., Crossley, C., Sridhar, R., Misra, H. P., Janzen, E. G., & McCay, P. B. (1986). In vivo spin trapping of free radicals generated in brain, spleen, and liver during γ radiation of mice. *Arch. Biochem. Biophys.*, 244(1), 156–160. [https://doi.org/10.1016/0003-9861\(86\)90104-9](https://doi.org/10.1016/0003-9861(86)90104-9)
 36. Lebel, C. P., Ischiropoulos, H., & Bondys, S. C. (1992). Evaluation of the Probe 2',7'-Dichlorofluorescein as an Indicator of Reactive Oxygen Species Formation and Oxidative Stress. *Chem. Res. Toxicol.*, 5(2), 227-231. <https://doi.org/10.1021/tx00026a012>
 37. Lowry, O. H., Rosebrough, N. J., Farr, A. L., & Randall, R. J. (1951). Protein measurement with the Folin phenol reagent. *J. Biol. Chem.*, 193(1), 265–275. [https://doi.org/10.1016/0304-3894\(92\)87011-4](https://doi.org/10.1016/0304-3894(92)87011-4)
 38. Lynn, S., Gurr, J. R., Lai, H. T., & Jan, K. Y. (2000). NADH Oxidase Activation Is Involved in Arsenite-Induced Oxidative DNA Damage in Human Vascular Smooth Muscle Cells. *Circ. Res.*, 86(5), 514–519. <https://doi.org/10.1161/01.RES.86.5.514>
 39. Marquez, L. A., & Dunford, H. B. (1995). Kinetics of oxidation of tyrosine and dityrosine by myeloperoxidase compounds I and II: Implications for lipoprotein peroxidation studies. *J. Biol. Chem.*, 270(51), 30434–30440. <https://doi.org/10.1074/jbc.270.51.30434>
 40. McDonald, C. C., Phillips, W. D., & Mower, H. F. (1965). An Electron Spin Resonance Study of Some Complexes of Iron, Nitric Oxide, and Anionic Ligands. *J. Am. Chem. Soc.*, 87(19), 9579–9591. <https://doi.org/10.1021/ja01093a007>
 41. Morton, W. E., & Caron, G. A. (1989). Encephalopathy: An uncommon manifestation of workplace arsenic poisoning? *Am. J. Ind. Med.*, 15(1), 1–5. <https://doi.org/10.1002/ajim.4700150102>
 42. Navoni, J., & Olivera, N. (2009). Optimización y validación metodológica de la cuantificación de arsénico por inyección en flujo-generación de hidruros- espectrometría de absorción atómica (if-gh-aea) previa derivatización con l-cisteína. *Acta Toxicol. Argent.*, 17(2), 15–25.
 43. Negishi, T., Matsunaga, Y., Kobayashi, Y., Hirano, S., & Tashiro, T. (2013). Developmental subchronic exposure to diphenylarsinic acid induced increased exploratory behavior, impaired learning behavior, and decreased cerebellar glutathione concentration in rats. *Toxicol. Sci.*, 136(2), 478–486. <https://doi.org/10.1093/toxsci/kft200>
 44. Pachauri, V., Mehta, A., Mishra, D., & Flora, S. J. S. (2013). Arsenic induced neuronal apoptosis in guinea pigs is Ca²⁺ dependent and abrogated by chelation therapy: Role of voltage gated calcium channels. *NeuroToxicology*, 35(1), 137–145. <https://doi.org/10.1016/j.neuro.2013.01.006>
 45. Pi, J., Kumagai, Y., Sun, G., Yamauchi, H., Yoshida, T., Iso, H., Endo, A., Yu, L., Yuki, K., Miyauchi, T., & Shimojo, N. (2000). Decreased serum concentrations of nitric oxide metabolites among Chinese in an endemic area of chronic arsenic poisoning in inner Mongolia. *Free Radical Biol. Med.*, 28(7), 1137–1142. [https://doi.org/10.1016/S0891-5849\(00\)00209-4](https://doi.org/10.1016/S0891-5849(00)00209-4)
 46. Prütz, W. A., Mönig, H., Butler, J., & Land, E. J. (1985). Reactions of nitrogen dioxide in aqueous model systems: Oxidation of tyrosine units in peptides and proteins. *Arch. Biochem. Biophys.*, 243(1), 125–134. [https://doi.org/10.1016/0003-9861\(85\)90780-5](https://doi.org/10.1016/0003-9861(85)90780-5)
 47. Radi, R. (2018). Oxygen radicals, nitric oxide, and peroxynitrite: Redox pathways in molecular medicine. *Proc. Nat. Acad. Sci. U. S. A.*, 115(23), 5839–5848. <https://doi.org/10.1073/pnas.1804932115>
 48. Ramezani, M. S., Padmaja, S., & Koppenol, W. H. (1996). Nitration and hydroxylation of phenolic compounds by peroxynitrite. *Chem. Res. Toxicol.*, 9(1), 232–240. <https://doi.org/10.1021/tx950135w>
 49. Saha, S., Sadhukhan, P., Mahalanobish, S., Dutta, S., & Sil, P. C. (2018). Ameliorative role of genistein against age-dependent chronic arsenic toxicity in murine brains via the regulation of oxidative stress and inflammatory

- signaling cascades. *J. Nutr. Biochem.*, 55, 26–40. <https://doi.org/10.1016/j.jnutbio.2017.11.010>
50. Sampson, J. B., Rosen, H., & Beckman, J. S. (1996). Peroxynitrite-dependent tyrosine nitration catalyzed by superoxide dismutase, myeloperoxidase, and horseradish peroxidase. *Methods Enzymol.*, 269, 210–218. [https://doi.org/10.1016/S0076-6879\(96\)69023-5](https://doi.org/10.1016/S0076-6879(96)69023-5)
 51. Shi, H., Shi, X., & Liu, K. J. (2004). Oxidative mechanism of arsenic toxicity and carcinogenesis. *Mol. Cell. Biochem.*, 255(1/2), 67–78. <https://doi.org/10.1023/B:MCBI.0000007262.26044.e8>
 52. Signes-Pastor, A. J., Vioque, J., Navarrete-Muñoz, E. M., Carey, M., García-Villarino, M., Fernández-Somoano, A., Tardón, A., Santa-Marina, L., Irizar, A., Casas, M., Guxens, M., Llop, S., Soler-Blasco, R., García-de-la-Hera, M., Karagas, M. R., & Meharg, A. A. (2019). Inorganic arsenic exposure and neuropsychological development of children of 4–5 years of age living in Spain. *Environ. Res.*, 174, 135–142. <https://doi.org/10.1016/j.envres.2019.04.028>
 53. Thomas, D. J., Waters, S. B., & Styblo, M. (2004). Elucidating the pathway for arsenic methylation. *Toxicol. Appl. Pharmacol.*, 198(3), 319–126. <https://doi.org/10.1016/j.taap.2003.10.020>
 54. von Bartheld, C. S., Bahney, J., & Herculano-Houzel, S. (2016). The search for true numbers of neurons and glial cells in the human brain: A review of 150 years of cell counting. *J. Comp. Neurol.*, 524(18), 3865–3895. <https://doi.org/10.1002/cne.24040>
 55. Wang, J. P., Qi, L., Moore, M. R., & Ng, J. C. (2002). A review of animal models for the study of arsenic carcinogenesis. *Toxicol. Lett.*, 133(1), 17–31. [https://doi.org/10.1016/S0378-4274\(02\)00086-3](https://doi.org/10.1016/S0378-4274(02)00086-3)
 56. Wu, M. M., Chiou, H. Y., Hsueh, Y. M., Hong, C. T., Su, C. L., Chang, S. F. (2006). Effect of plasma homocysteine level and urinary monomethylarsonic acid on the risk of arsenic-associated carotid atherosclerosis. *Toxicol. Appl. Pharmacol.*, 216, 168-75.
 57. Zarazúa, S., Pérez-Severiano, F., Delgado, J. M., Martínez, L. M., Ortiz-Pérez, D., & Jiménez-Capdeville, M. E. (2006). Decreased nitric oxide production in the rat brain after chronic arsenic exposure. *Neurochem. Res.*, 31(8), 1069–1077. <https://doi.org/10.1007/s11064-006-9118-7>.